Supplementary Information

Fluorine-free binder-based dry thick electrodes with Parafilm® M for sustainable and efficient battery manufacturing

Min Kyung Kim[a,b,c,†], Taegyun Yu[a, †], Sungbin Jang[a,d, †], Juho Lee[a,e], Min Jang[a,e], Hyeseong Oh[e], Hyungyeon Cha[a], Huiyeol Lee[b], Joonhee Kang[b], Seung Min Lee[a,e], Hyeong-Seok Shim[a], Kwon-Hyung Lee[a], Gyujin Song[a], Wooyoung Jin[a], Tae-Hee Kim[a], Sinho Choi[a], Kyeong-Min Jeong[e], Joong Tark Han[f,g], Jung-Keun Yoo[h], Hun-Gi Jung[h] Sanghyun Song[i], Myoungkeon Park[i], Jinwoo Seong[i], Dongoh Kim[i], Hyunwoo Choi[j], Minjong Seong[j], Min Jin Lim[j], Wook Ryol Hwang[j,k], Jieun Nam[l], Sanghoon Jo[l], Jinsoo Kim[a,c,*]

[a] Ulsan Advanced Energy Technology R&D Center, Korea Institute of Energy Research, Ulsan, Republic of Korea

[b] Department of Nano Fusion Technology, Pusan National University, Busan, Republic of Korea

[c] Department of Energy Science and Engineering, Daegu Gyeongbuk Institute of Science & Technology (DGIST), Daegu, Republic of Korea

[d] Department of Organic Material Science and Engineering, Pusan National University, Busan, Republic of Korea

[e] Department of Energy Engineering, School of Energy and Chemical Engineering, Ulsan National Institute of Science and Technology (UNIST), Ulsan, Republic of Korea

[f] Nano Hybrid Technology Research Center, Creative and Fundamental Research Division, Korea Electrotechnology Research Institute (KERI), Changwon, Republic of Korea

[g] Department of Electro-Functionality Materials Engineering, University of Science and Technology (UST), Changwon, Republic of Korea

[h] Energy Storage Research Center, Korea Institute of Science and Technology (KIST), Seoul, Republic of Korea

[i] R&D Center, Rechargeable Battery Division, Hanwha Momentum, Seongnam, Republic of Korea

[j] School of Mechanical Engineering, Gyeongsang National University, Jinju, Republic of Korea

[k] R&D Center, Yunsung F&C Co., Ltd., Anseong, Republic of Korea

[l] Multiphysics Digital Twin Lab, Trinity Engineering, Seoul, Republic of Korea

* Email addresses of corresponding authors: jkim@kier.re.kr (J. Kim)

Keywords: fluorine-free binder, paraffin, dry electrode, thick electrode, lithium-ion batteries

Supplementary Table 1. Assignment of FT-IR characteristic peaks

Bonding	Wavenumber (cm^{-1})
CF_2	612
CH_2 rocking	719
C-F	1175
CF_3	1213
C-H	1396
-CH=CH- stretching	1462
	1472
$-CH_2$ stretching	2847
	2915
$-CH_3$ stretching	2952

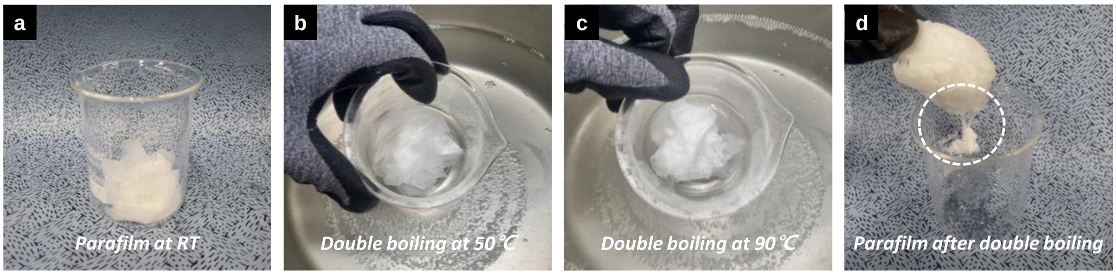

Supplementary Fig. 1. Physical changes of Parafilm at the temperature around 90 °C.

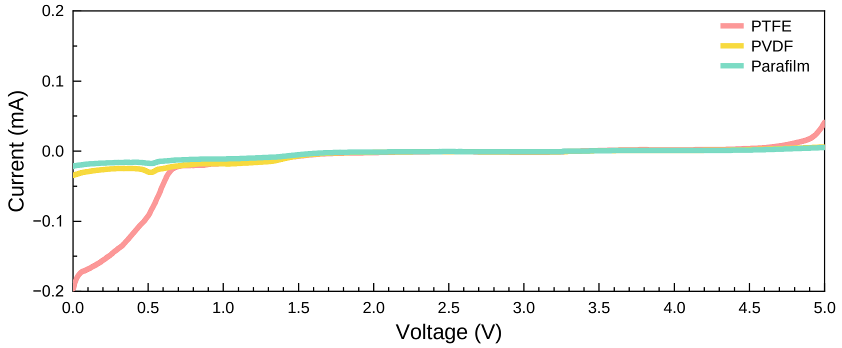

Supplementary Fig. 2. Reduction and oxidation stability of binder in Li|binder film cells tested by linear sweep voltammetry(LSV) at a scan rate of 1mV s^{-1}.

Supplementary Table 2. Volume and mass ratios according to binder.

Binder Type		Unit	Material			
			Active material	Conductive agent	Binder	Sum
PTFE	Material true density	g/cc	4.76	1.95	2.10	-
	Gravimetric composition	wt%	96	2	**2**	100.00
	Volumetric composition	vol%	91.07	4.63	4.30	100.00
PVDF	Material true density	g/cc	4.76	1.95	1.80	-
	Gravimetric composition	wt%	96	2	**2**	100.00
	Volumetric composition	vol%	90.42	4.60	4.98	100.00
Parafilm	Material true density	g/cc	4.76	1.95	0.98	-
	Gravimetric composition	wt%	96	2	**2**	100.00
	Volumetric composition	vol%	86.80	4.41	8.78	100.00
	Material true density	g/cc	4.76	1.95	0.98	-
	Gravimetric composition	wt%	97	2	**1**	100.00
	Volumetric composition	vol%	90.88	4.57	4.55	100.00

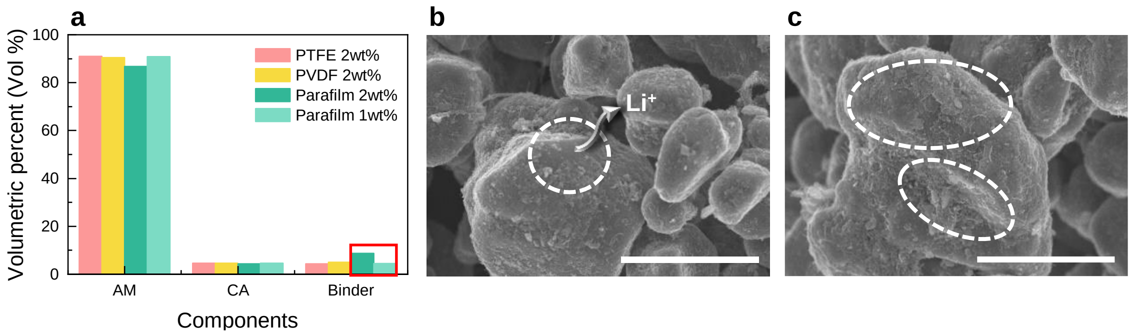

Supplementary Fig. 3. Parafilm mixed powder at various volume ratios. a **V**ariation in **v**olume **r**atio with **d**ifferent **m**ass **f**ractions of **v**arious **b**inders**.** SEM **i**mages of **a**ctive **m**aterial **p**article **s**urfaces with **b** 1 wt% and **c** 2 wt% Parafilm **b**inder **a**ddition**.** The scale bar represents 5 μm.

Supplementary Table 3. Comparison of adhesion strength using peel-off test of the electrode between this work and other references.

Electrode			Loading (mg cm^{-2})	Adhesion strength (N cm^{-1})
This study	Dry coating Electrode	Parafilm	50	5.9
		PTFE	50	-
	Wet coating Electrode	PVDF	50	-
Reference	Dry coating Electrode(PTFE) (NCM622/CNT/binder = 92/5/3)		30	4.6
	Wet coating Electrode (PVDF) (NCM811/carbon black additive/binder = 92/3/5)		40	2.3
			60	0

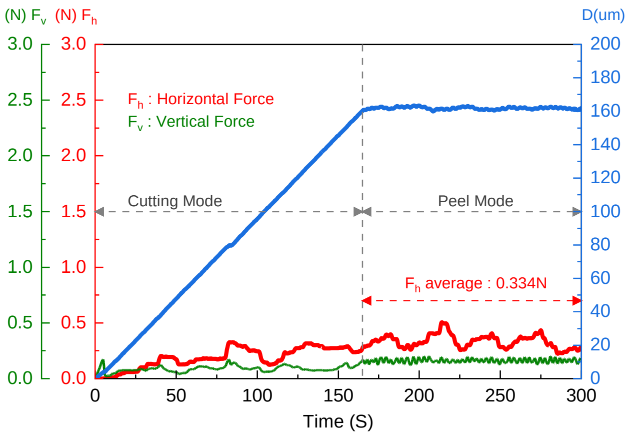

Supplementary Fig. 4. Representative force/depth profiles measured by SAICAS. Analysis of adhesion properties of Parafilm-based electrode.

Supplementary Table 4. Comparison of adhesion strength using SAICAS of the electrode between this work and other references.

Electrode		Loading (mAh cm^{-2})	Adhesion strength (N)
This work	Dry coating Electrode(Parafilm)	8	0.334
Reference	Dry coating Electrode (PTFE) (SC-NCA/LPSCl/CNF/PTFE = 85/13/1/1)	3	0.6
	Wet double coating Electrode (PVDF) (NCM622/carbon conductor/PVDF = 93/3/4)	3.5	0.04~0.05

Supplementary Table 5. Comparison of physical properties according to coating method.

Ø14 Electrode (40 mg cm^{-2}, 3.3~3.4 g/cc)	Wet Coating (PVDF binder)	Dry Coating (Parafilm binder)
Folding Test		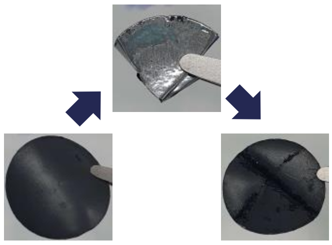
Wettability Test	20.51 ° 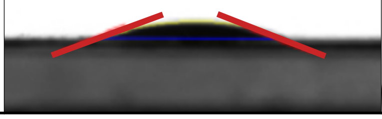	17.76 ° 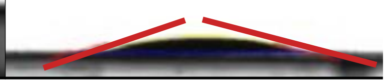

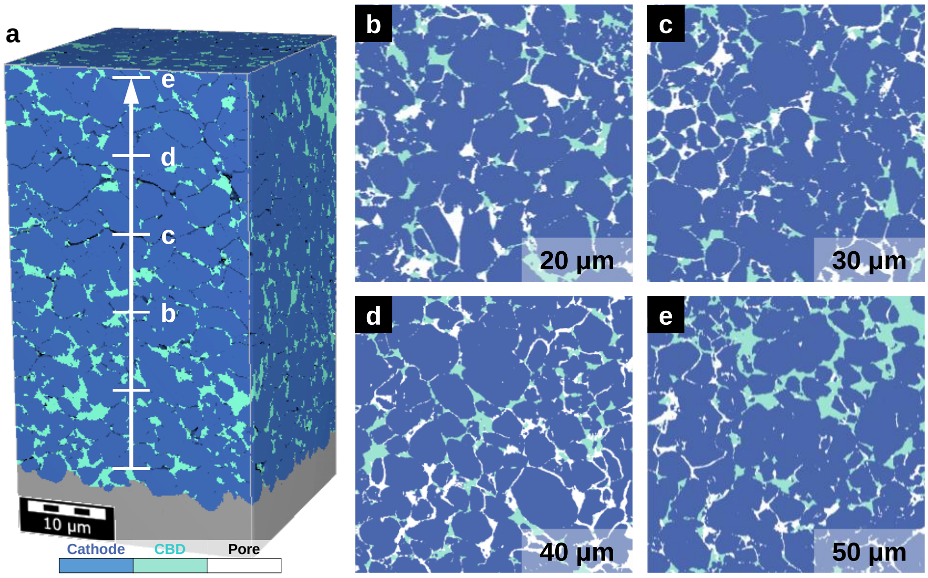

Supplementary Fig. 5. 3D FIB-SEM reconstructions of the Parafilm-based electrode. a Reconstructed 3D volume of the electrode. Sliced 2D images at **b** 20, **c** 30, **d** 40, and **e** 50 µm through thickness direction.

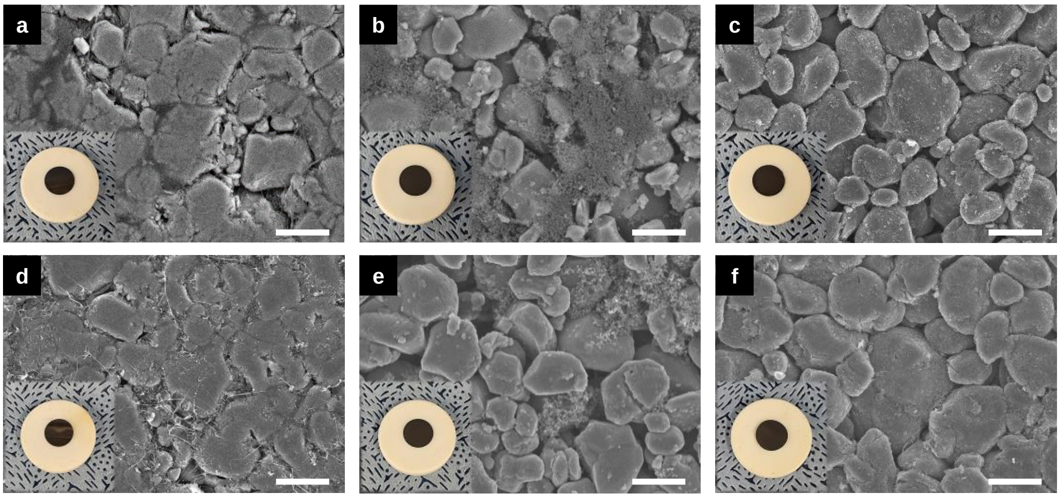

Supplementary Fig. 6. SEM image of the surface morphology of electrode. The inserted picture is a photograph of the electrode surface. On the surface of the electrode use each **a** PTFE, **b** PVDF, and **c** Parafilm binders before scorching test. **d** PTFE, **e** PVDF, and **f** Parafilm binders after scorching test. The scale bars represents 10 μm.

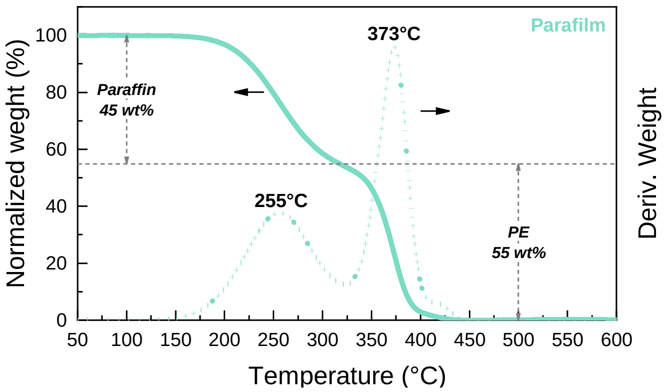

Supplementary Fig. 7. TGA curves of Parafilm binder.

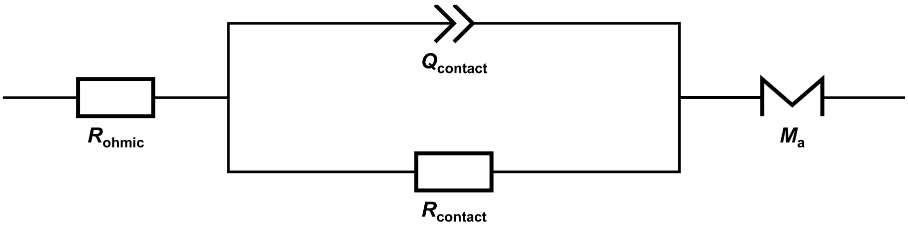

R_{ohmic} : ohmic resistance

$R_{contact}$: contact resistance

$Q_{contact}$: contact constant phase element

M_a : modified restricted diffusion

Supplementary Fig. 8. Equivalent circuit model for fitting impedance spectra.

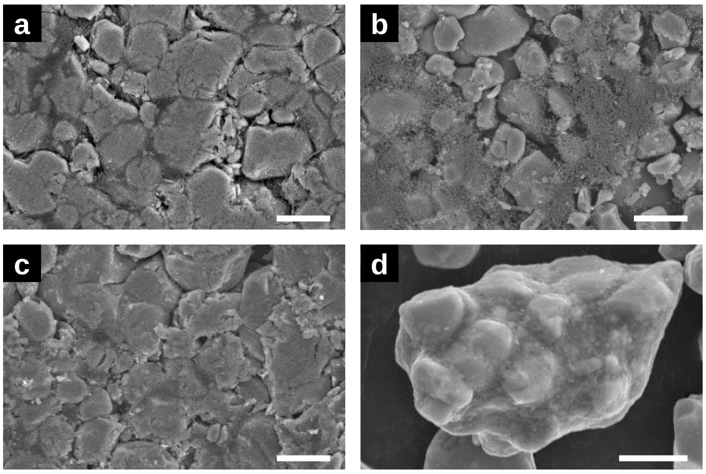

Supplementary Fig. 9. SEM image of the surface morphology of electrodes. On the surface of the electrode use each **a** PTFE, **b** PVDF, and **c** Parafilm binders before the formation cycle. The scale bars are 10 μm. **d** Zoom in on the powder mixed with the parafilm binder (Scale bar: 2 μm).

Supplementary Table 6. The parameters for ionic tortuosity calculation.

K_{bulk} (S/cm)			Surface (cm^2)		
0.0077			1.5394		
Binder	**Thickness (cm)**	**Porosity**	**R_{ion} (Ω)**	**R_{ion} ($Ω.cm^2$)**	**Tortuosity**
PTFE	0.0172	0.1956	53.62	85.54	7.23
PVDF	0.0243	0.3589	90.88	139.90	15.91
Parafilm	0.0167	0.1874	39.15	60.27	5.21

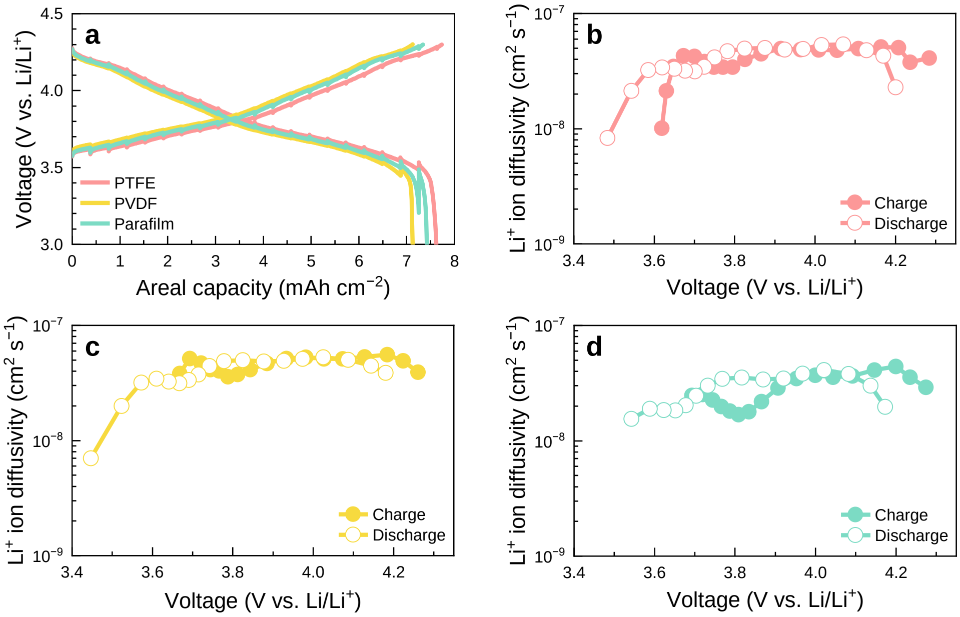

Supplementary Fig. 10. GITT profiles of each binder and corresponding diffusion coefficient. **a** GITT cycle data for voltage as a function of areal capacity. Calculated diffusion coefficient ($\boldsymbol{D_{Li^+}}$) of the half cell using **b** PTFE, **c** PVDF, and **d** Parafilm from the GITT for charge/discharge.

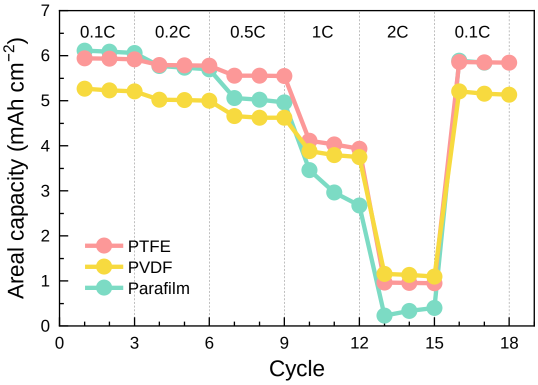

Supplementary Fig. 11. Rate performance of half cell using different binders in the voltage range of 3.0-4.3V. Charge/discharge at rates of C/10, C/5, C/2, 1C, 2C, and the back to C/10.

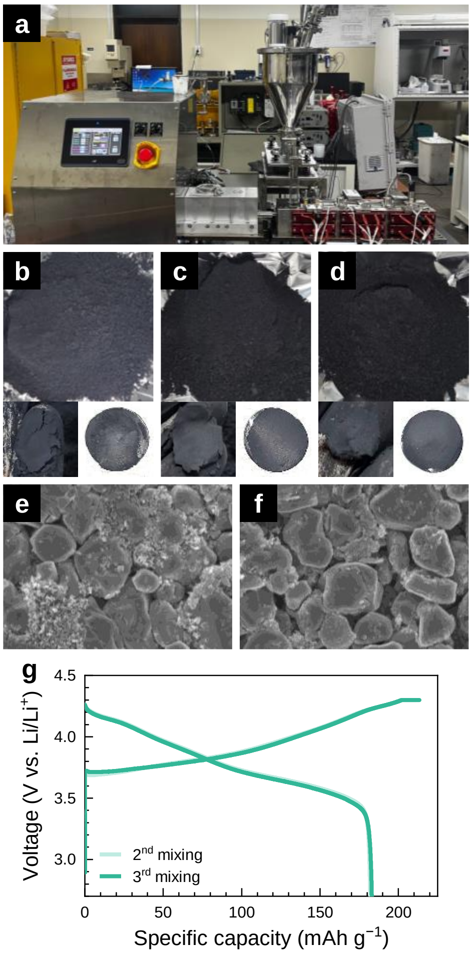

Supplementary Fig. 12. Twin-screw-based continuous dry mixing process with Parafilm binder. Photographs of **a** continuous twin-screw mixer, and the dry mixed powder with the iteration of **b** first, **c** second, and **d** third. The left-bottom insets show the hand-clumped dry mixed powder, and the right-bottom ones show the fabricated dry electrodes. The microstructure with dry mixing iterations of **e** second and **f** third. **g** The initial electrochemical profiles of the second and third mixed dry electrode powder.

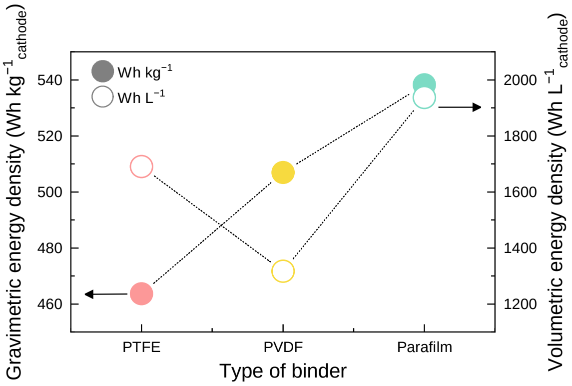

Supplementary Fig. 13. The gravimetric energy density and volumetric energy density of coin cells with different binders.

Supplementary Table 7. Initial charge/discharge capacities and columbic efficiencies for NCM811 with each binder half coin cells (40 mg cm^{-2}, 0.1C) and NCM811/graphite full coin cells (40 mg cm^{-2}, 0.3C).

Cell type	Cell number	Charge capacity (mAh cm^{-2})	Average charge capacity (mAh cm^{-2})	Discharge capacity (mAh cm^{-2})	Average discharge capacity (mAh cm^{-2})	Columbic efficiency (%)	Average coulombic efficiency (%)
NCM811 with PTFE half-coin cells	1	8.634		7.859		90.902	
	2	8.664	8.444	7.920	7.706	91.288	91.186
	3	8.033		7.340		91.369	
NCM811 with PVDF half-coin cells	1	8.487		6.824		80.297	
	2	7.619	7.540	6.670	6.649	87.423	88.891
	3	6.515		6.453		98.952	
NCM811 with Parafilm half-coin cells	1	8.432		7.502		88.843	
	2	8.552	8.527	7.733	7.658	90.421	89.726
	3	8.596		7.739		89.915	
NCM811 with PTFE /graphite full-coin cells	1	7.251		5.872		80.979	
	2	8.484	8.058	5.870	6.063	69.191	75.523
	3	8.439		6.447		76.400	
NCM811 with PVDF /graphite full-coin cells	1	7.208		6.396		88.728	
	2	7.572	7.078	6.670	6.529	88.087	91.922
	3	6.453		6.522		98.952	
NCM811 with Parafilm /graphite full-coin cells	1	7.337		6.582		89.715	
	2	6.924	7.207	6.121	6.428	88.409	89.183
	3	7.536		7.443		89.424	

Supplementary Table 8. The mass loading, density, and capacity loading of NCM811 electrode using Parafilm binder and graphite electrode.

Electrode Type	Mass ratio (%)	Mass loading (mg cm^{-2})	Density (g cm^{-3})	Capacity loading (mAh cm^{-2})	N/P ratio
NCM811	AM/SP/CNT/Parafilm =97/1.5/0.5/1	37.8	3.8	7.33	1.05
graphite	AM/SP/SBR/CMC =95/2/1.5/1.5	22.4	1.04	7.66	

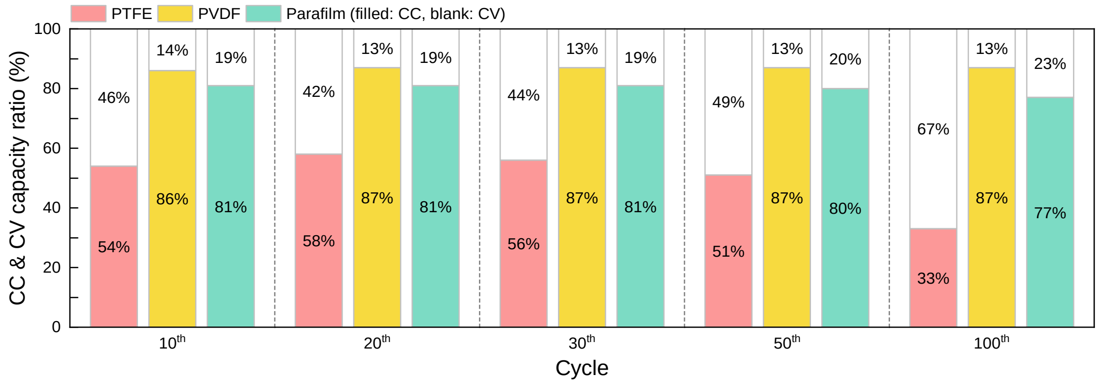

Supplementary Fig. 14. Comparison of CC and CV mode charge capacities with each binder after the 10th, 20th, 30th, 50th, and 100th cycles.

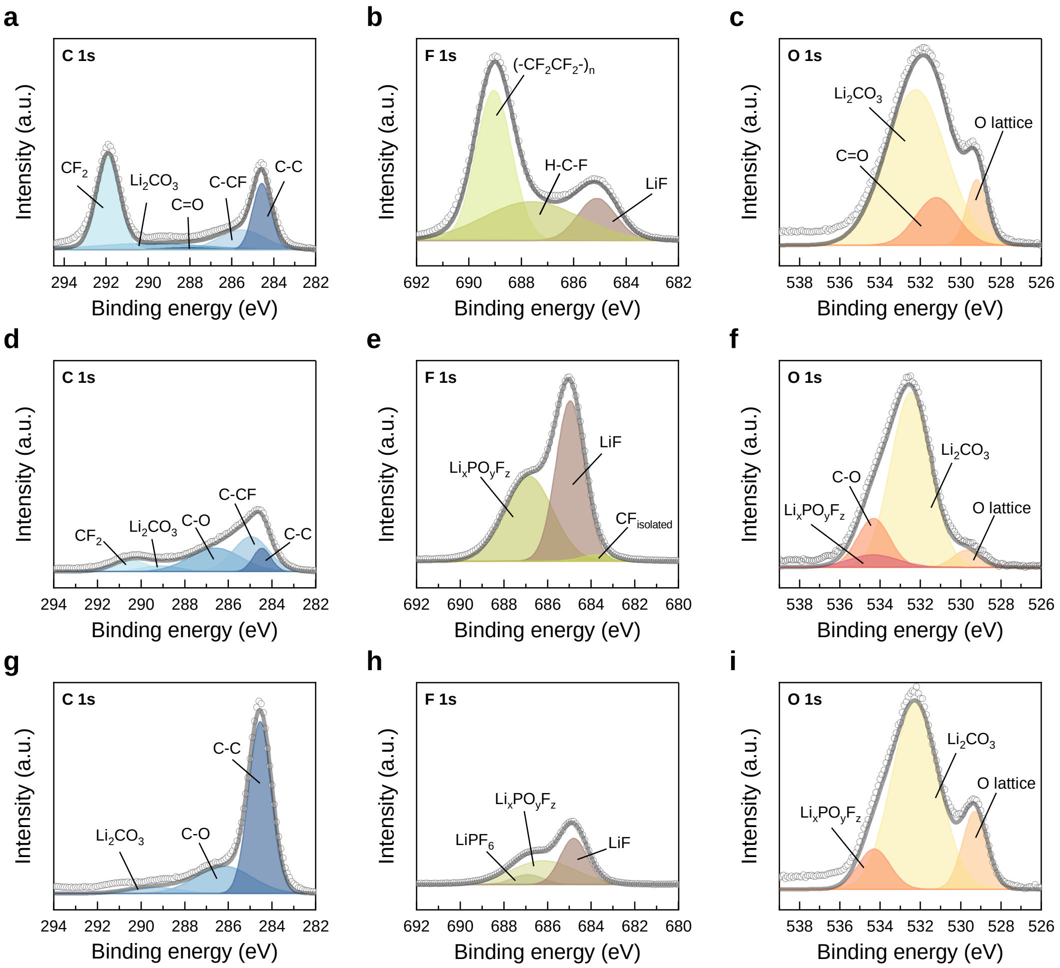

Supplementary Fig. 15. XPS analysis of the CEI layers on the formation cycled NCM811 cathode surface. C 1s, F 1s, and O 1s XPS spectra of the **a-c** PTFE, **d-f** PVDF, and **g-i** Parafilm.

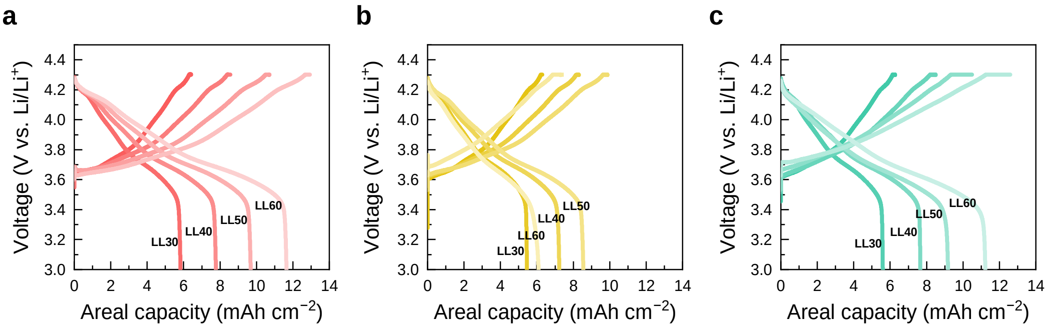

Supplementary Fig. 16. Formation voltage profile. At areal mass loading 30, 40, 50, and 60mg cm^{-2} for **a** PTFE, **b** PVDF, and **c** parafilm half cell in the voltage range of 3.0-4.3V at 0.1C.

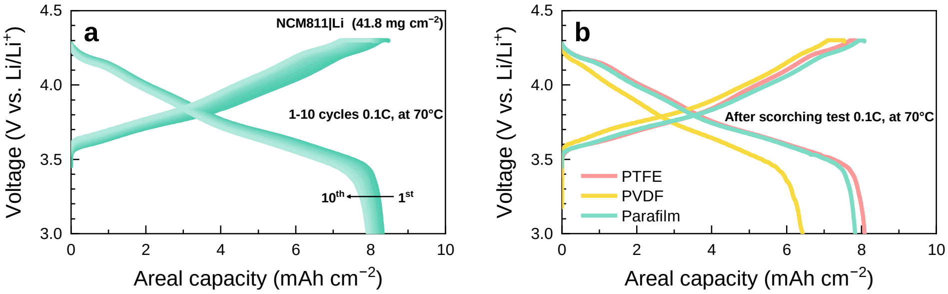

Supplementary Fig. 17. Cycle data for thermal stability verification. a Voltage profile of Parafilm-based cell at 70°C above T_g for 10 cycles. **b** Cycle voltage profiles of the electrodes after scorching test.

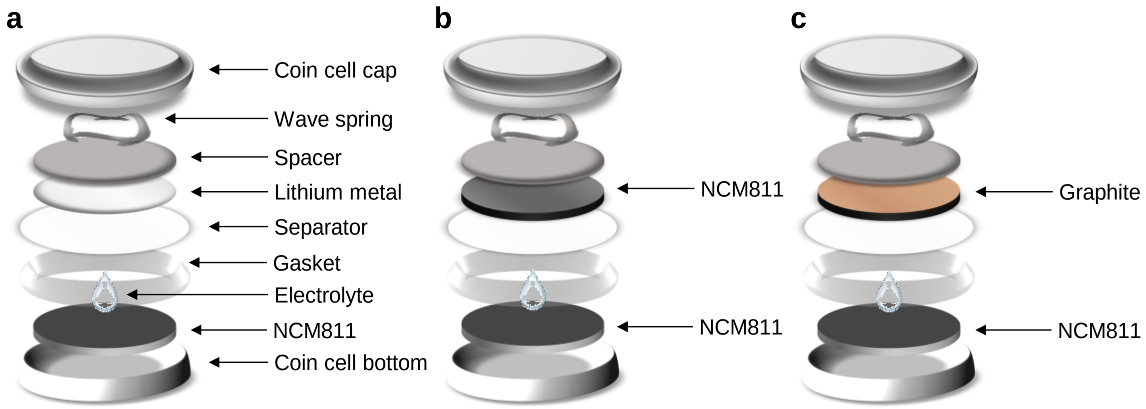

Supplementary Fig. 18. Coin cell architecture. **a** NCM811|Li half coin cell **b** NCM811|NCM811 Symmetric cell **c** NCM811|Graphite full coin cell.